STRUCTURAL CHEMISTRY

ISSN 2053-2296

Structural and spectroscopic characterization of a new luminescent Ni^{II} complex: bis{2,4-dichloro-6-[(2-hydroxypropyl)iminomethyl]phenolato-κ^3O,N,O'}nickel(II)

Duygu Akin Kara,[a] Adem Donmez,[a,b] Hulya Kara[a,c]* and M. Burak Coban[c,d]*

[a]Department of Physics, Molecular Nano-Materials Laboratory, Mugla Sitki Kocman University, Mugla, Turkey, [b]Scientific Research Projects Coordination Unit, Mugla Sitki Kocman University, Mugla, Turkey, [c]Department of Physics, Balikesir University, Balikesir, Turkey, and [d]Center of Sci and Tech App and Research, Balikesir University, Balikesir, Turkey. *Correspondence e-mail: karahulya04@gmail.com, burakcoban@balikesir.edu.tr

Received 13 February 2018
Accepted 25 June 2018

Edited by T.-B. Lu, Sun Yat-Sen University, People's Republic of China

Keywords: nickel(II) complex; Schiff base; crystal structure; photoluminescence; green light emitting devices.

CCDC reference: 1589491

Supporting information: this article has supporting information at journals.iucr.org/c

The design and preparation of transition-metal complexes with Schiff base ligands are of interest due to their potential applications in the fields of molecular magnetism, nonlinear optics, dye-sensitized solar cells (DSSCs), sensing and photoluminescence. Luminescent metal complexes have been suggested as potential phosphors in electroluminescent devices. A new luminescent nickel(II) complex, $[Ni(C_{10}H_{10}Cl_2NO_2)_2]$, has been synthesized and characterized by single-crystal X-ray diffraction and elemental analysis, UV–Vis, FT–IR, ^1H NMR, ^{13}C NMR and photoluminescence spectroscopies, and LC–MS/MS. Molecules of the complex in the crystals lie on special positions, on crystallographic binary rotation axes. The Ni^{II} atoms are six-coordinated by two phenolate O, two imine N and two hydroxy O atoms from two tridentate Schiff base 2,4-dichloro-6-[(2-hydroxypropyl)iminomethyl]phenolate ligands, forming an elongated octahedral geometry. Furthermore, the complex exhibits a strong green luminescence emission in the solid state at room temperature, as can be seen from the (CIE) chromaticity diagram, and hence the complex may be a promising green OLED (organic light-emitting diode) in the development of electroluminescent materials for flat-panel-display applications.

1. Introduction

During the last decade, transition-metal complexes have been of great interest since they have potential applications in coordination chemistry, catalysis and sensors, and display biological and magnetic properties (Sherino *et al.*, 2018; Bang *et al.*, 2016; Vittaya *et al.*, 2017; Hajikhanmirzaei *et al.*, 2015; Vamja & Surati, 2017; Keypour *et al.*, 2017). Recently, Schiff base ligands and their metal complexes have attracted attention as organic photovoltaic materials since their use as potential substitutes for dye-sensitized solar cells (DSSCs) (Zhang *et al.*, 2018; Yang *et al.*, 2010; Wesley Jeevadason *et al.*, 2014; Dinçalp *et al.*, 2010). In addition, impressive progress has been made in the photophysical and optoelectronic applications of these complexes, because they exhibit photoluminescence (PL), as well as electroluminescence (EL), and these qualities point to potential applications in the development of energy-efficient low-cost full-colour and flat-panel OLED (organic light-emitting diode) displays (Nishal *et al.*, 2014, 2015; Taghi Sharbati *et al.*, 2011; Yan *et al.*, 2018; Bizzarri *et al.*, 2017). Zn^{II}, Pd^{II}, Pt^{II}, Ir^{III} and Re^{I} complexes have been much more studied as luminescence emitters in comparison with Ni^{II} complexes (Li *et al.*, 2013; Lepeltier *et al.*, 2015; Singh *et al.*, 2016; Nishal *et al.*, 2015; Bizzarri *et al.*, 2017). Therefore,

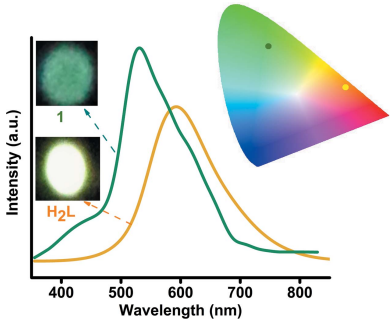

Ni^{II} complexes do not appear as numerously in the literature as emitter materials for OLEDs. However, some recent articles have evidenced an increasing interest for emitting Ni^{II} complexes (Srinivas *et al.*, 2016; Cerezo *et al.*, 2017; More *et al.*, 2017*b*). In the last decade, our research group and others have reported the synthesis, structural, spectroscopic, NLO and magnetic properties of some nickel(II) Schiff base complexes (Elerman *et al.*, 2001; Kara *et al.*, 2003; Ünver *et al.*, 2006; Shawish *et al.*, 2016; Elmehdawi *et al.*, 2017). According to the Cambridge Structural Database (CSD, Version 5.38, November 2016 updates; Groom *et al.*, 2016), there are few reports on investigations of the emission spectra of salen-type ligands [salen is 2,2′-ethylenebis(nitrilomethylidene)diphenol] and their Ni^{II} complexes (More *et al.*, 2017*a*,*b*; Donmez *et al.*, 2017*a*,*b*). Green emitting materials provide one of the prime colours in the development of full-colour display technology and there is still a big challenge in developing emission materials to display green light. In this context, in view of the importance of luminescent Ni^{II} complexes and in an effort to enlarge the library of such complexes, a new luminescent nickel(II) complex, namely bis{2,4-dichloro-6-[(2-hydroxypropyl)iminomethyl]phenolato-κ^3O,N,O'}nickel(II), (1), has been synthesized and characterized by single-crystal X-ray diffraction and elemental analysis, solid-state UV–Vis, FT–IR, ^{1}H NMR, ^{13}C NMR and solid-state photoluminescence spectroscopies, and LC–MS/MS.

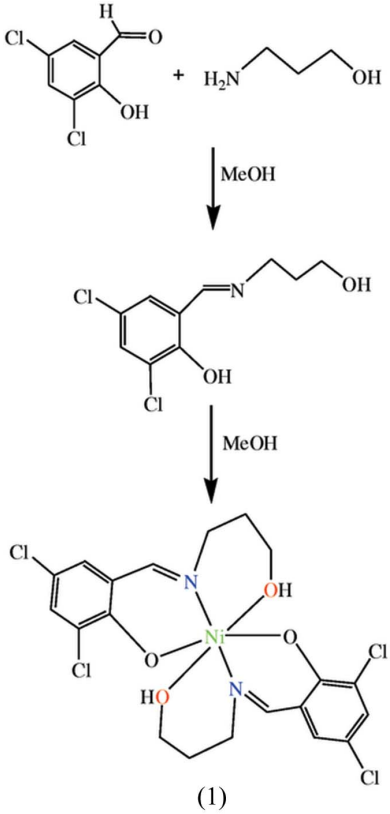

(1)

Scheme 1

2. Experimental

All chemicals and solvents used for the synthesis were of reagent grade and were used without further purification. Elemental analyses (C, H and N) were carried out by standard methods. The solid-state UV–Vis spectra were determined with an Ocean Optics Maya 2000 Pro Spectrometer (250–600 nm). The FT–IR spectra were measured with a Perkin-Elmer Spectrum 65 instrument in the range 4000–600 cm^{-1}. The solid-state luminescence spectra in the visible region were measured at room temperature with an ANDOR SR500i-BL photoluminescence spectrometer equipped with a triple grating and using an air-cooled CCD camera as the detector. The measurements were carried out using the excitation source (349 nm) of a Spectra-physics Nd:YLF laser with a 5 ns pulse width and 1.3 mJ of energy per pulse as the source. Mass spectra were determined with an LC–MS/MS AB Sciex Qtrap 5500 instrument. The ^{1}H and ^{13}C NMR spectra of the free Schiff base ligand were recorded [in dimethyl sulfoxide (DMSO)] using a Bruker Ultrashield Plus Biospin (400 MHz) instrument. Powder X-ray diffraction (PXRD) patterns were recorded on a Bruker D8 Advance diffractometer using Cu $K\alpha$ radiation (λ = 1.5418 Å) in the range $5 < 2\theta < 50°$ in θ–θ mode with a step of n s ($5 < n < 10$ s) and a step width of 0.03°. A comparison between the experimental and calculated (from the CIF) PXRD patterns was performed with the *Mercury* program (Macrae *et al.*, 2008).

2.1. Synthesis and crystallization

A solution of 3-aminopropan-1-ol (1 mmol, 0.075 g) in methanol (10 ml) was added slowly to a solution of 3,5-dichlorosalicylaldehyde (1 mmol, 0.191 g) in methanol (20 ml). The mixture was stirred for 1 h at 330 K. The yellow product of 2,4-dichloro-6-[(2-hydroxypropyl)iminomethyl]phenol (H_2L) precipitated from the solution on cooling (yield 82%). Elemental analysis calculated for $C_{10}H_{11}Cl_2NO_2$ (%): C 48.41, H 4.47, N 5.65; found: C 48.36, H 4.49, N 5.63. LS–MS/MS *m*/*z* found 248.0, requires 248.1 (see Fig. S3 in the supporting information). ^{1}H NMR (400 MHz, DMSO-d_6, Me_4Si, ppm): δ 8.56 (*s*, 1H, HC═N), 7.55 (*d*, *J* = 2.8 Hz, 1H, aromatic), 7.40 (*d*, *J* = 2.4 Hz, 1H, aromatic), 4.68 (*brs*, 1H, OH), 3.72 (*t*, *J* = 6.8 Hz, 2H, H_2C—N), 3.51 (*t*, *J* = 6.0 Hz, 2H, H_2C—OH), 1.82 (quint, *J* = 6.4, 10.4 Hz, 2H, aliphatic methylene). ^{13}C NMR (100 MHz, DMSO-d_6, Me_4Si, ppm): δ 165.33 (**C**═N), 163.54 (**C**═C═O), 132.72 (aromatic), 130.22 (aromatic), 124.57 (**C**═C—Cl), 116.76 (**C**═C—O), 57.83 (methylene), 50.94 (H_2C—OH), 32.61 (H_2C—N). See Figs. S1 and S2 in the supporting information for the NMR spectra.

Complex (1) was prepared by the addition of a solution of nickel(II) acetate tetrahydrate (0.249 g, 1 mmol) in methanol (30 ml) to a solution of H_2L (1 mmol, 0.248 g) in methanol (30 ml). The resulting solution was stirred for 2 h at 333 K and then filtered. The filtrate was left to stand at room temperature. After two weeks, single crystals were obtained (yield 44%). The synthetic route for the preparation of H_2L and (1) is outlined in Scheme 1. Analysis calculated for $C_{20}H_{20}Cl_4N_2NiO_4$ (%): C 43.45, H 3.65, N 5.07; found: C 43.11, H 3.67, N 5.08. LS–MS/MS *m*/*z* found 553.3, requires 552.9 (see Fig. S4 in the supporting information).

Table 1
Experimental details.

Crystal data	
Chemical formula	$[Ni(C_{10}H_{10}Cl_2NO_2)_2]$
M_r	552.89
Crystal system, space group	Monoclinic, *C*2/*c*
Temperature (K)	292
a, *b*, *c* (Å)	20.5375 (19), 10.7332 (6), 22.4073 (19)
β (°)	108.073 (10)
V (Å^3)	4695.6 (7)
Z	8
Radiation type	Mo $K\alpha$
μ (mm^{-1})	1.31
Crystal size (mm)	0.32 × 0.21 × 0.17
Data collection	
Diffractometer	Agilent Xcalibur Eos
Absorption correction	Analytical [*CrysAlis PRO* (Rigaku OD, 2015), based on expressions derived by Clark & Reid (1995)]
T_{min}, T_{max}	0.521, 0.685
No. of measured, independent and observed [$I > 2\sigma(I)$] reflections	7742, 4420, 3127
R_{int}	0.032
(sin $\theta/\lambda)_{max}$ (Å^{-1})	0.610
Refinement	
$R[F^2 > 2\sigma(F^2)]$, $wR(F^2)$, S	0.051, 0.129, 1.09
No. of reflections	4420
No. of parameters	287
No. of restraints	2
H-atom treatment	H atoms treated by a mixture of independent and constrained refinement
$\Delta\rho_{max}$, $\Delta\rho_{min}$ (e Å^{-3})	0.96, −0.48

Computer programs: *CrysAlis PRO* (Rigaku OD, 2015), *SHELXT* (Sheldrick, 2015*a*), *SHELXL2016* (Sheldrick, 2015*b*) and *OLEX2* (Dolomanov *et al.*, 2009).

2.2. Refinement

Crystal data, data collection and structure refinement details for complex (1) are summarized in Table 1. H-atom positions were calculated geometrically and refined using a riding model, except for the hydroxy H atoms, for which their positional parameters were refined with restraints [0.84 (2) Å] applied to the O—H distances.

3. Results and discussion

3.1. Crystal structure

Molecules of complex (1) in the crystal lie on special positions, on crystallographic binary rotation axes, and have crystallographic *C*2 point symmetry (Fig. 1). The crystallographically independent unit contains two independent half molecules. The Ni^{II} atom is six-coordinated by two phenolate O, two imine N and two hydroxy O atoms from two tridentate Schiff base ligands, forming a slightly elongated octahedral geometry. The Ni—O bond lengths range from 2.029 (3) to 2.106 (3) Å and the Ni—N distances are 2.060 (3) and 2.053 (3) Å. The *trans* angles at the Ni atom are in the range 173.47 (11)–176.86 (19)°, while the other angles are close to 90°, ranging from 84.44 (16) to 96.02 (12)°, indicating a slightly distorted octahedral coordination. Selected bond lengths and angles are listed in Table 2, and are typical and comparable

Table 2
Selected geometric parameters (Å, °).

Ni1—O1	2.096 (3)	Ni2—O3	2.041 (3)
Ni1—O2	2.029 (3)	Ni2—O4	2.106 (3)
Ni1—N1	2.060 (3)	Ni2—N2	2.053 (3)
O1^i—Ni1—O1	86.70 (16)	O3—Ni2—O3^i	94.75 (15)
O2—Ni1—O1	175.92 (11)	O3—Ni2—O4^i	90.54 (11)
O2^i—Ni1—O1	89.59 (11)	O3—Ni2—O4	173.47 (11)
O2^i—Ni1—O2	94.17 (15)	O3—Ni2—N2^i	96.02 (12)
O2—Ni1—N1^i	94.59 (12)	O3—Ni2—N2	86.57 (12)
O2—Ni1—N1	87.55 (12)	O4—Ni2—O4^i	84.44 (16)
N1—Ni1—O1^i	87.15 (13)	N2—Ni2—O4^i	88.10 (13)
N1—Ni1—O1	90.57 (13)	N2—Ni2—O4	89.08 (13)
N1^i—Ni1—N1	176.86 (19)	N2^i—Ni2—N2	176.19 (19)

Symmetry code: (i) $-x+1, y, -z+\frac{3}{2}$.

with those observed in nickel(II) Schiff base complexes (Wang *et al.*, 2011; Zhou *et al.*, 2009; Ayikoé *et al.*, 2011). In the crystal structure of (1), the aliphatic –OH group of the tridentate Schiff base ligand actively participates in intermolecular O—H···O hydrogen bonds, connecting to one other unit and resulting in a one-dimensional chain along the *b* axis (Fig. 2 and Table 3). The intramolecular Ni1···Ni2 distance is 5.346 (3) Å and the intermolecular Ni2···Ni1^{ii} [symmetry code: (ii) x, $y-1$, z] distance is 5.388 (3) Å in the chain structure (Fig. 2). The shortest intermolecular Cl···Cl contact is Cl2···Cl4^{iii} of 3.443 (3) Å [symmetry code: (iii) $x+\frac{1}{2}, -y+\frac{3}{2}, z-\frac{1}{2}$], which connects the molecules into a two-dimensional structure in the *bc* plane (Fig. 3).

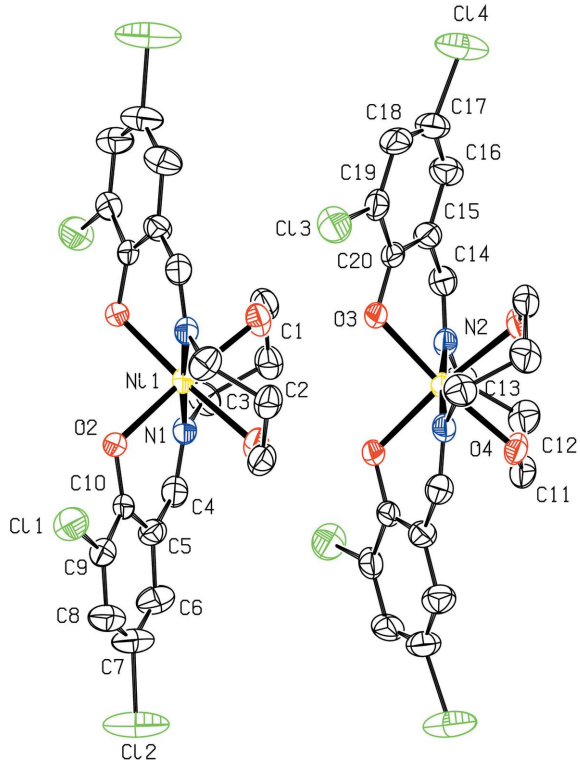

Figure 1
The molecular structure of (1), showing the atom-labelling scheme and drawn with 50% probability displacement ellipsoids. [Symmetry code: (i) $-x, -y+1, -z+1$.]

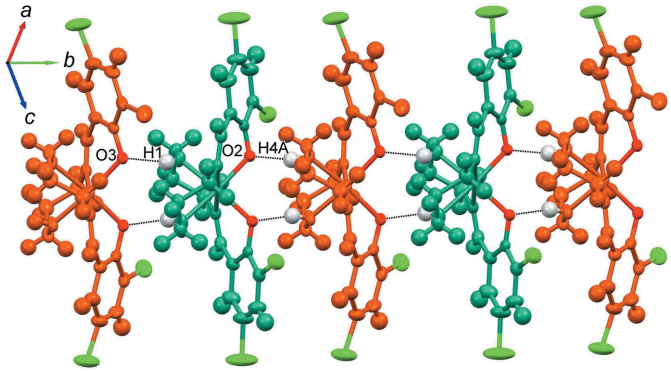

Figure 2
The one-dimensional hydrogen-bonded chain structure in (1). Dotted lines indicate O—H···O hydrogen bonds. Generic atom labels without symmetry codes have been used. See Table 3 for hydrogen-bond details.

3.2. Powder X-ray diffraction pattern

Before proceeding to the spectroscopic and photoluminescence studies, we also carried out a powder X-ray diffraction (PXRD) experiment to investigate the purity of (1). The PXRD results showed that the peak positions match well with those from the simulated PXRD patterns on the basis of single-crystal structure data, indicating reasonable crystalline phase purity (Fig. 4).

3.3. Spectroscopy

The FT–IR spectrum of (1) is consistent with the structural characteristics determined by single-crystal X-ray diffraction (Fig. 5). By comparing the IR spectra of H_2L and its complex (1), the coordination modes and the parts of the ligand bound to the metal ion were explored. On coordination, the stretching vibrations for the ν(C═N) and ν(C—O) bonds show a significant shift from 1648 to 1633 cm^{-1} and from 1204 to 1167 cm^{-1} for H_2L and (1), respectively (Coban *et al.*, 2018; Donmez *et al.*, 2017*a*). The absorptions between 2964 and 2855 cm^{-1} are characteristic of the C—H aromatic and aliphatic stretching vibrations for both structures (Kocak *et al.*, 2017). The broad band attributed to the existence of a ν(O—H) stretching vibration at 3231 cm^{-1} of H_2L was

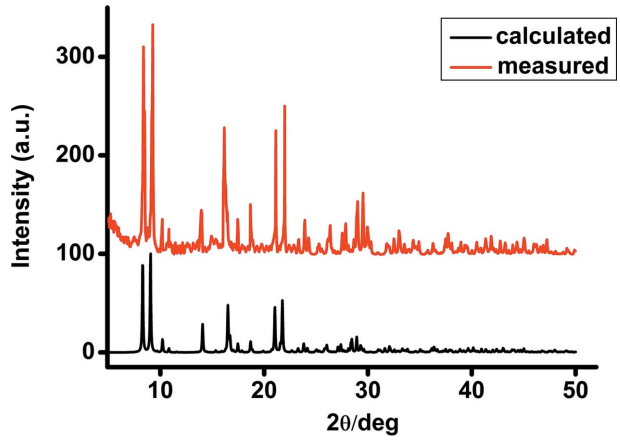

Figure 4
Powder X-ray diffraction pattern of (1). The black line represents the pattern simulated from the CIF and the red line represents the experimental pattern.

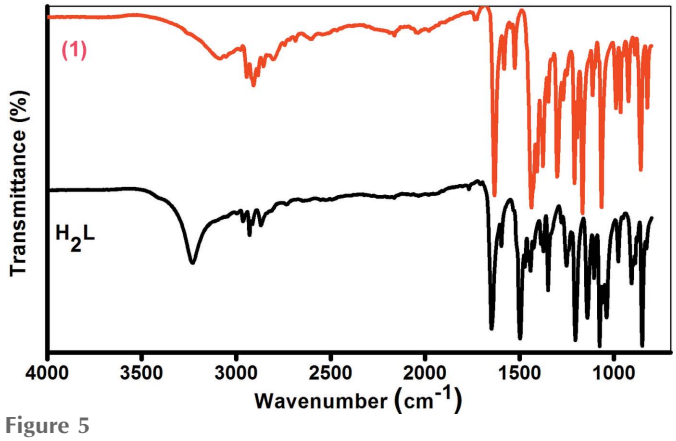

Figure 5
The IR spectra of H_2L (black line) and (1) (red line).

Table 3
Hydrogen-bond geometry (Å, °).

D—H···*A*	*D*—H	H···*A*	*D*···*A*	*D*—H···*A*
O1—H1···O3	0.84 (3)	1.87 (3)	2.702 (4)	172 (4)
O4—H4*A*···O2^{ii}	0.84 (2)	1.91 (2)	2.736 (4)	168 (4)

Symmetry code: (ii) $x, y-1, z$.

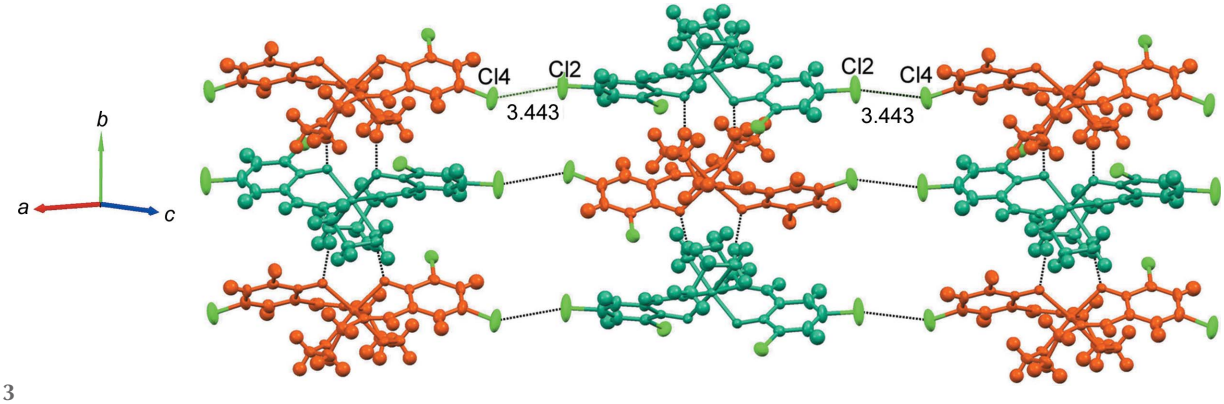

Figure 3
A crystal packing view of the polymeric networks in the *bc* plane showing the intermolecular Cl···Cl interactions (dotted lines). Generic atom labels without symmetry codes have been used.

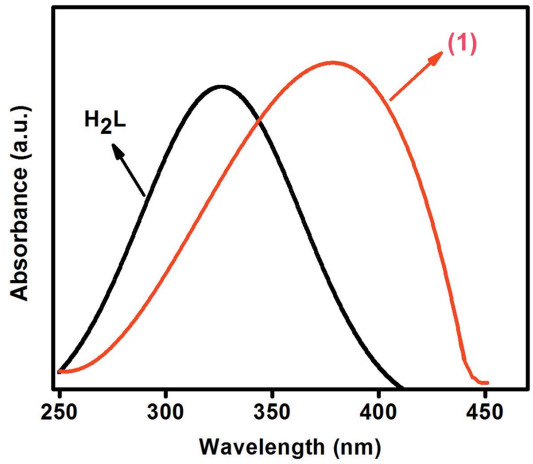

Figure 6
The solid-state UV–Vis spectra of H_2L (black line) and (1) (red line).

replaced by the weaker broad band at 3085 cm^{-1} after metal and ligand complexation (Yahsi *et al.*, 2016*a*). The shift of the peak position of the hydroxy groups and the broadening of the band could be attributed to the formation of the metal complex. The ν(C—Cl) stretching vibrations from the 3,5-chlorobenzene rings are observed between 858 and 824 cm^{-1} in H_2L and (1), respectively (Donmez *et al.*, 2017*b*).

The photophysical properties of H_2L and (1) have been reported through solid-state UV–Vis absorption (Fig. 6) and solid-state photoluminescence spectroscopy (Fig. 7). The similarity in the shapes of the absorption and emission bands suggests that the bands result from ligand-centred transitions. As shown in the solid-state UV–Vis spectrum in Fig. 6, H_2L displays an essential broad band in the UV region (λ_{max} = 263 nm), which may be attributed to ligand-centred $\pi\rightarrow\pi^*$ and $n\rightarrow\pi^*$ transitions (Gliemann, 1985; Celen *et al.*, 2013; Yahsi *et al.*, 2016*b*). On the other hand, the absorption spectrum of (1) is characterized by a broad band (λ_{max} = 381 nm), which shifts towards lower energy upon complexation.

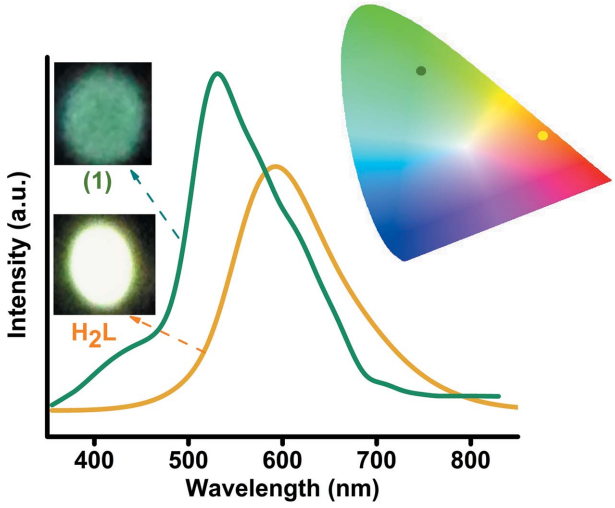

Figure 7
The emission spectra of H_2L (yellow line) and (1) (green line) in solid samples at room temperature (λ_{ex} = 349 nm). The upper left and lower left photos are luminescence images of (1) and H_2L, respectively. The upper right inset is a CIE colour space chromaticity diagram of the H_2L (yellow circle) and complex (1) (green circle) emissions.

The solid-state photoluminescence spectra of free H_2L and (1) were investigated at room temperature upon excitation at λ_{ex} = 349 nm. As shown in Fig. 7, H_2L displays a broad yellow emission band at λ_{max} = 592 nm, with CIE coordinates of 0.55 and 0.41, which can be attributed to $\pi\rightarrow\pi^*$ electronic transitions in the molecular orbital manifolds of the aromatic ring systems of the ligand, suggesting that there may be intraligand charge transfer (ILCT) (Coban *et al.*, 2016, 2018; Oylumluoglu *et al.*, 2017). The occurrence of a photo-induced electron transfer (PET) process may be responsible for quenching the luminescence of the ligand, depending on the presence of a lone pair of electrons on the N- and O-donor atoms in the ligand (Shafaatian *et al.*, 2015; Basak *et al.*, 2007). Complex (1) displays an intense green broad emission band occurring at λ_{max} = 526 nm, with CIE coordinates of 0.22 and 0.62 in the visible region. The intensity of the emission in (1) is greater than that of the free ligand (H_2L). The main reason for this is that the PET process was prevented by the complexation of the ligand to the metal ion. Therefore, the luminescence intensity may be greatly increased by the coordination of the Ni^{II} atom (Hopa & Cokay, 2016). In addition, chelation of H_2L to the Ni^{II} atom increases the rigidity of the HL^- ligand and thus reduces energy loss through thermal vibration decay (Das *et al.*, 2006). However, the increase of luminescence by complexation is very interesting because it creates opportunities for the photochemical applications of these complexes (Majumder *et al.*, 2006). Upon coordinating to the Ni^{II} atom, the observed blue shift (66 nm) of the emission maximum between free H_2L and its complex (1) may be denoted as CHEF (chelation-enhanced fluorescence) (Song *et al.*, 2015; Erkarslan *et al.*, 2016).

4. Conclusion

The compound characterized in this study is a new example of a nickel(II) Schiff base complex which shows luminescence in the green region of the spectrum. Our results show that the emission band in the complex displays a blue shift and a greater intensity than that of the free organic ligand (H_2L) when excited at 349 nm. The blue shift and enhanced luminescence intensity for the complex may be due to the chelation of the ligand to the metal centre. Such chelation enhances the rigidity of the ligand and thus reduces the loss of energy by radiationless decay of the intraligand emission excited state. The CIE graph indicated that this phosphor might be very useful for green-light-emitting diodes and solid-state lighting applications.

Acknowledgements

The authors are grateful to Dokuz Eylul University for the use of the Agilent Xcalibur Eos diffractometer (purchased under University Research grant No. 2010.KB.FEN.13) and Balikesir University, Science and Technology Application and Research Center (BUBTAM) for the use of the mass and photo-

luminescence spectrometers. The authors also thank Dr Muhittin Aygun (Dokuz Eylul University) for the X-ray measurement and Dr Erhan Kaplaner (Mugla Sıtkı Kocman University) for NMR comments.

Funding information

Funding for this research was provided by: Research Funds of Mugla Sitki Kocman University (grant No. BAP-2017/029).

References

Ayikoé, K., Gultneh, Y. & Butcher, R. J. (2011). *Acta Cryst.* E**67**, m1211.
Bang, S., Kim, J., Jang, B. W., Kang, S.-G. & Kwak, C. H. (2016). *Inorg. Chim. Acta*, **444**, 176–180.
Basak, S., Sen, S., Banerjee, S., Mitra, S., Rosair, G. & Rodriguez, M. T. G. (2007). *Polyhedron*, **26**, 5104–5112.
Bizzarri, C., Spuling, E., Knoll, D. M., Volz, D. & Bräse, S. (2017). *Coord. Chem. Rev.* https://doi.org/10.1016/j.ccr.2017.09.011.
Celen, S., Gungor, E., Kara, H. & Azaz, A. D. (2013). *J. Coord. Chem.* **66**, 3170–3181.
Cerezo, J., Requena, A., Zúñiga, J., Piernas, M. J., Santana, M. D., Pérez, J. & García, L. (2017). *Inorg. Chem.* **56**, 3663–3673.
Clark, R. C. & Reid, J. S. (1995). *Acta Cryst.* A**51**, 887–897.
Coban, M. B., Erkarslan, U., Oylumluoglu, G., Aygun, M. & Kara, H. (2016). *Inorg. Chim. Acta*, **447**, 87–91.
Coban, M. B., Gungor, E., Kara, H., Baisch, U. & Acar, Y. (2018). *J. Mol. Struct.* **1154**, 579–586.
Das, D., Chand, B. G., Sarker, K. K., Dinda, J. & Sinha, C. (2006). *Polyhedron*, **25**, 2333–2340.
Dinçalp, H., Yavuz, S., Haklı, Ö., Zafer, C., Özsoy, C., Durucasu, İ. & İçli, S. (2010). *J. Photochem. Photobiol. Chem.* **210**, 8–16.
Dolomanov, O. V., Bourhis, L. J., Gildea, R. J., Howard, J. A. K. & Puschmann, H. (2009). *J. Appl. Cryst.* **42**, 339–341.
Donmez, A., Coban, M. B., Kocak, C., Oylumluoglu, G., Baisch, U. & Kara, H. (2017*a*). *Mol. Cryst. Liq. Cryst.* **652**, 213–222.
Donmez, A., Oylumluoglu, G., Coban, M. B., Kocak, C., Aygun, M. & Kara, H. (2017*b*). *J. Mol. Struct.* **1149**, 569–575.
Elerman, Y., Kara, H., Prout, K. & Chippindale, A. (2001). *Acta Cryst.* C**57**, 149–150.
Elmehdawi, R., EL-Kaheli, M., Abuhmaiera, R., Treish, F., Ben Younes, M., Bazzicalupi, C., Guerri, A., Caneschi, A. & Amjad, A. (2017). *Materials (Basel)*, **10**, article number 178.
Erkarslan, U., Oylumluoglu, G., Coban, M. B., Öztürk, E. & Kara, H. (2016). *Inorg. Chim. Acta*, **445**, 57–61.
Gliemann, G. (1985). *Ber. Bunsen. Phys. Chem.* **89**, 99–100.
Groom, C. R., Bruno, I. J., Lightfoot, M. P. & Ward, S. C. (2016). *Acta Cryst.* B**72**, 171–179.
Hajikhanmirzaei, L., Safaei, E., Wojtczak, A. & Jagličić, Z. (2015). *Inorg. Chim. Acta*, **430**, 125–131.
Hopa, C. & Cokay, I. (2016). *Acta Cryst.* C**72**, 601–606.
Kara, H., Elerman, Y. & Elmali, A. (2003). *Z. Naturforsch. B*, **58**, 955–958.
Keypour, H., Shayesteh, M., Rezaeivala, M., Dhers, S., Küp, F. Ö., Öztürk, İ, Güllü, M. & Ng, S. (2017). *J. Mol. Struct.* **1148**, 568–576.
Kocak, C., Oylumluoglu, G., Donmez, A., Coban, M. B., Erkarslan, U., Aygun, M. & Kara, H. (2017). *Acta Cryst.* C**73**, 414–419.
Lepeltier, M., Morlet-Savary, F., Graff, B., Lalevée, J., Gigmes, D. & Dumur, F. (2015). *Synth. Met.* **199**, 139–146.
Li, K., Cheng, G., Ma, C., Guan, X., Kwok, W.-M., Chen, Y., Lu, W. & Che, C.-M. (2013). *Chem. Sci.* **4**, 2630–2644.
Macrae, C. F., Bruno, I. J., Chisholm, J. A., Edgington, P. R., McCabe, P., Pidcock, E., Rodriguez-Monge, L., Taylor, R., van de Streek, J. & Wood, P. A. (2008). *J. Appl. Cryst.* **41**, 466–470.
Majumder, A., Rosair, G. M., Mallick, A., Chattopadhyay, N. & Mitra, S. (2006). *Polyhedron*, **25**, 1753–1762.
More, M. S., Devkule, S. S. & Chavan, S. S. (2017*a*). *J. Fluoresc.* **27**, 841–851.
More, M. S., Pawal, S. B., Lolage, S. R. & Chavan, S. S. (2017*b*). *J. Mol. Struct.* **1128**, 419–427.
Nishal, V., Singh, D., Kumar, A., Tanwar, V., Singh, I., Srivastava, R. & Kadyan, P. S. (2014). *J. Org. Semicond.* **2**, 15–20.
Nishal, V., Singh, D., Saini, R. K., Tanwar, V., Kadyan, S., Srivastava, R. & Kadyan, P. S. (2015). *Cogent Chem.* **1**, 1–10.
Oylumluoglu, G., Coban, M. B., Kocak, C., Aygun, M. & Kara, H. (2017). *J. Mol. Struct.* **1146**, 356–364.
Rigaku OD (2015). *CrysAlis PRO*. Rigaku Oxford Diffraction Ltd, Yarnton, Oxfordshire, England.
Shafaatian, B., Hashemibagha, M., Notash, B. & Rezvani, S. A. (2015). *J. Organomet. Chem.* **791**, 51–57.
Shawish, H. B., Maah, M., Halim, S. N. A. & Shaker, S. A. (2016). *Arab. J. Chem.* **9**, S1935–S1942.
Sheldrick, G. M. (2015*a*). *Acta Cryst.* A**71**, 3–8.
Sheldrick, G. M. (2015*b*). *Acta Cryst.* C**71**, 3–8.
Sherino, B., Mohamad, S., Abdul Halim, S. N. & Abdul Manan, N. S. (2018). *Sens. Actuators B Chem.* **254**, 1148–1156.
Singh, D., Bhagwan, S., Saini, R. K., Nishal, V. & Singh, I. (2016). *Advanced Magnetic and Optical Materials*, edited by A. Tiwari, P. K. Iyer, V. Kumar & H. Swart, pp. 473–519. Hoboken, NJ, USA: John Wiley & Sons Inc.
Song, X.-Q., Peng, Y.-Q., Cheng, G.-Q., Wang, X.-R., Liu, P.-P. & Xu, W.-Y. (2015). *Inorg. Chim. Acta*, **427**, 13–21.
Srinivas, M., Shrungesh Kumar, T. O., Mahadevan, K. M., Naveen, S., Vijayakumar, G. R., Nagabhushana, H., Kumara, M. N. & Lokanath, N. K. (2016). *J. Sci. Adv. Mater. Dev.* **1**, 324–329.
Taghi Sharbati, M., Soltani Rad, M. N., Behrouz, S., Gharavi, A. & Emami, F. (2011). *J. Lumin.* **131**, 553–558.
Ünver, H., Elmali, A., Karakaş, A., Kara, H. & Donmez, E. (2006). *J. Mol. Struct.* **800**, 18–22.
Vamja, A. C. & Surati, K. R. (2017). *Luminescence*, **32**, 1197–1202.
Vittaya, L., Leesakul, N., Saithong, S. & Phongpaichit, S. (2017). *ScienceAsia*, **43**, 175–185.
Wang, C. Y., Li, J. F., Wang, P. & Yuan, C. J. (2011). *Acta Cryst.* **E67**, m1227–m1228.
Wesley Jeevadason, A., Kalidasa Murugavel, K. & Neelakantan, M. A. (2014). *Renew. Sustain. Energy Rev.* **36**, 220–227.
Yahsi, Y., Gungor, E., Coban, M. B. & Kara, H. (2016*a*). *Mol. Cryst. Liq. Cryst.* **637**, 67–75.
Yahsi, Y., Ozbek, H., Aygun, M. & Kara, H. (2016*b*). *Acta Cryst.* C**72**, 426–431.
Yan, L., Li, R., Shen, W. & Qi, Z. (2018). *J. Lumin.* **194**, 151–155.
Yang, S., Kou, H., Wang, H., Cheng, K. & Wang, J. (2010). *New J. Chem.* **34**, 313–317.
Zhang, J., Xu, L. & Wong, W. Y. (2018). *Coord. Chem. Rev.* **355**, 180–198.
Zhou, T., Zhou, R.-J. & An, Z. (2009). *Acta Cryst.* E**65**, m779.

supporting information

Acta Cryst. (2018). C**74**, 901-906 [https://doi.org/10.1107/S2053229618009166]

Structural and spectroscopic characterization of a new luminescent Ni^{II} complex: bis{2,4-dichloro-6-[(2-hydroxypropyl)iminomethyl]phenolato-κ^3O,N,O'}nickel(II)

Duygu Akin Kara, Adem Donmez, Hulya Kara and M. Burak Coban

Computing details

Data collection: *CrysAlis PRO* (Rigaku OD, 2015); cell refinement: *CrysAlis PRO* (Rigaku OD, 2015); data reduction: *CrysAlis PRO* (Rigaku OD, 2015); program(s) used to solve structure: SHELXT (Sheldrick, 2015a); program(s) used to refine structure: *SHELXL2016* (Sheldrick, 2015b); molecular graphics: OLEX2 (Dolomanov *et al.*, 2009); software used to prepare material for publication: OLEX2 (Dolomanov *et al.*, 2009).

Bis{2,4-dichloro-6-[(2-hydroxypropyl)iminomethyl]phenolato-κ^3O,N,O'}nickel(II)

Crystal data

$[Ni(C_{10}H_{10}Cl_2NO_2)_2]$
M_r = 552.89
Monoclinic, $C2/c$
a = 20.5375 (19) Å
b = 10.7332 (6) Å
c = 22.4073 (19) Å
β = 108.073 (10)°
V = 4695.6 (7) Å^3
Z = 8
$F(000)$ = 2256
D_x = 1.564 Mg m^{-3}
Mo $K\alpha$ radiation, λ = 0.71073 Å
Cell parameters from 2317 reflections
θ = 3.7–28.1°
μ = 1.31 mm^{-1}
T = 292 K
Prism, green
0.32 × 0.21 × 0.17 mm

Data collection

Xcalibur, Eos diffractometer
Detector resolution: 8.0667 pixels mm^{-1}
ω scans
Absorption correction: analytical [CrysAlis PRO (Rigaku OD, 2015), based on expressions derived by Clark & Reid (1995)]
T_{min} = 0.521, T_{max} = 0.685
7742 measured reflections
4420 independent reflections
3127 reflections with $I > 2\sigma(I)$
R_{int} = 0.032
θ_{max} = 25.7°, θ_{min} = 3.2°
h = −24→22
k = −13→10
l = −27→16

Refinement

Refinement on F^2
Least-squares matrix: full
$R[F^2 > 2\sigma(F^2)]$ = 0.051
$wR(F^2)$ = 0.129
S = 1.09
4420 reflections
287 parameters
2 restraints
Hydrogen site location: mixed
H atoms treated by a mixture of independent and constrained refinement
$w = 1/[\sigma^2(F_o^2) + (0.0441P)^2 + 4.9249P]$ where $P = (F_o^2 + 2F_c^2)/3$
$(\Delta/\sigma)_{max}$ = 0.001
$\Delta\rho_{max}$ = 0.96 e Å^{-3}
$\Delta\rho_{min}$ = −0.48 e Å^{-3}

Special details

Geometry. All esds (except the esd in the dihedral angle between two l.s. planes) are estimated using the full covariance matrix. The cell esds are taken into account individually in the estimation of esds in distances, angles and torsion angles; correlations between esds in cell parameters are only used when they are defined by crystal symmetry. An approximate (isotropic) treatment of cell esds is used for estimating esds involving l.s. planes.

Fractional atomic coordinates and isotropic or equivalent isotropic displacement parameters (Å²)

	x	*y*	*z*	U_{iso}*/U_{eq}
Ni1	0.500000	0.94958 (7)	0.750000	0.0279 (2)
Cl1	0.54771 (7)	1.15988 (12)	0.94460 (5)	0.0517 (3)
Cl2	0.30179 (8)	1.0281 (2)	0.96063 (7)	0.1007 (7)
O1	0.50449 (16)	0.8076 (3)	0.68720 (13)	0.0367 (7)
O2	0.49229 (14)	1.0783 (2)	0.81378 (12)	0.0313 (7)
N1	0.39456 (18)	0.9443 (3)	0.71840 (15)	0.0320 (8)
C1	0.4526 (2)	0.7924 (4)	0.62759 (19)	0.0428 (12)
H1A	0.461837	0.717088	0.607678	0.051*
H1B	0.454575	0.862248	0.600710	0.051*
C2	0.3824 (2)	0.7847 (4)	0.6339 (2)	0.0428 (12)
H2A	0.382276	0.721245	0.664696	0.051*
H2B	0.350644	0.758498	0.594005	0.051*
C3	0.3569 (2)	0.9072 (5)	0.6535 (2)	0.0456 (12)
H3A	0.361152	0.972646	0.625136	0.055*
H3B	0.308672	0.898814	0.649568	0.055*
C4	0.3588 (2)	0.9615 (4)	0.7555 (2)	0.0376 (10)
H4	0.312089	0.945846	0.739480	0.045*
C5	0.3846 (2)	1.0033 (4)	0.82048 (19)	0.0346 (10)
C6	0.3394 (2)	0.9951 (5)	0.8565 (2)	0.0488 (13)
H6	0.296078	0.960868	0.838905	0.059*
C7	0.3588 (3)	1.0369 (5)	0.9168 (2)	0.0542 (14)
C8	0.4222 (3)	1.0881 (5)	0.9440 (2)	0.0487 (13)
H8	0.435033	1.115878	0.985345	0.058*
C9	0.4666 (2)	1.0977 (4)	0.90923 (19)	0.0362 (10)
C10	0.4498 (2)	1.0594 (4)	0.84608 (18)	0.0311 (10)
Ni2	0.500000	0.45155 (7)	0.750000	0.0275 (2)
Cl3	0.70002 (6)	0.66331 (13)	0.74089 (7)	0.0579 (4)
Cl4	0.67063 (8)	0.42402 (18)	0.52341 (7)	0.0819 (6)
O3	0.55891 (14)	0.5803 (2)	0.72366 (13)	0.0326 (7)
O4	0.44015 (15)	0.3063 (3)	0.76858 (14)	0.0375 (7)
N2	0.44185 (18)	0.4452 (3)	0.65718 (16)	0.0330 (8)
C11	0.3686 (2)	0.2922 (4)	0.7356 (2)	0.0405 (11)
H11A	0.343523	0.360106	0.746926	0.049*
H11B	0.352385	0.214891	0.748466	0.049*
C12	0.3541 (2)	0.2912 (4)	0.6655 (2)	0.0454 (12)
H12A	0.306440	0.269108	0.645841	0.054*
H12B	0.381921	0.227162	0.654872	0.054*
C13	0.3682 (2)	0.4154 (4)	0.6385 (2)	0.0432 (12)
H13A	0.350323	0.412019	0.593009	0.052*

H13B	0.344280	0.481296	0.652679	0.052*
C14	0.4702 (2)	0.4524 (4)	0.6140 (2)	0.0368 (10)
H14	0.442685	0.436358	0.573133	0.044*
C15	0.5413 (2)	0.4833 (4)	0.6228 (2)	0.0361 (10)
C16	0.5688 (2)	0.4496 (5)	0.5754 (2)	0.0454 (12)
H16	0.541716	0.407314	0.540169	0.054*
C17	0.6345 (3)	0.4778 (5)	0.5800 (2)	0.0481 (13)
C18	0.6749 (2)	0.5468 (5)	0.6297 (2)	0.0476 (13)
H18	0.719243	0.569347	0.631525	0.057*
C19	0.6479 (2)	0.5818 (4)	0.6768 (2)	0.0404 (11)
C20	0.5815 (2)	0.5497 (4)	0.6766 (2)	0.0330 (10)
H4A	0.459 (2)	0.237 (3)	0.779 (2)	0.050*
H1	0.519 (2)	0.737 (2)	0.701 (2)	0.050*

Atomic displacement parameters (Å²)

	U^{11}	U^{22}	U^{33}	U^{12}	U^{13}	U^{23}
Ni1	0.0350 (4)	0.0194 (4)	0.0314 (4)	0.000	0.0134 (3)	0.000
Cl1	0.0576 (8)	0.0540 (8)	0.0434 (6)	−0.0137 (7)	0.0157 (6)	−0.0060 (6)
Cl2	0.0610 (10)	0.197 (2)	0.0597 (9)	−0.0077 (12)	0.0411 (8)	−0.0009 (11)
O1	0.048 (2)	0.0244 (16)	0.0356 (16)	0.0037 (15)	0.0094 (14)	−0.0045 (14)
O2	0.0381 (17)	0.0251 (16)	0.0369 (15)	−0.0040 (13)	0.0205 (13)	−0.0028 (12)
N1	0.039 (2)	0.0244 (18)	0.0339 (19)	0.0011 (17)	0.0125 (16)	0.0013 (16)
C1	0.058 (3)	0.035 (3)	0.035 (2)	0.004 (2)	0.015 (2)	−0.004 (2)
C2	0.048 (3)	0.035 (3)	0.043 (3)	−0.004 (2)	0.011 (2)	−0.009 (2)
C3	0.045 (3)	0.048 (3)	0.039 (3)	0.006 (2)	0.006 (2)	−0.006 (2)
C4	0.033 (2)	0.030 (2)	0.048 (3)	−0.001 (2)	0.012 (2)	0.001 (2)
C5	0.037 (3)	0.035 (2)	0.035 (2)	0.003 (2)	0.0146 (19)	0.007 (2)
C6	0.036 (3)	0.065 (3)	0.048 (3)	−0.002 (3)	0.017 (2)	0.009 (3)
C7	0.050 (3)	0.080 (4)	0.042 (3)	0.004 (3)	0.028 (2)	0.010 (3)
C8	0.051 (3)	0.062 (3)	0.039 (3)	0.006 (3)	0.023 (2)	0.004 (2)
C9	0.042 (3)	0.031 (2)	0.038 (2)	−0.001 (2)	0.015 (2)	0.003 (2)
C10	0.043 (3)	0.021 (2)	0.034 (2)	0.005 (2)	0.018 (2)	0.0039 (19)
Ni2	0.0255 (4)	0.0198 (4)	0.0404 (4)	0.000	0.0148 (3)	0.000
Cl3	0.0381 (7)	0.0510 (8)	0.0892 (10)	−0.0115 (6)	0.0265 (7)	−0.0143 (7)
Cl4	0.0729 (10)	0.1293 (16)	0.0606 (9)	0.0225 (10)	0.0454 (8)	0.0049 (9)
O3	0.0335 (17)	0.0225 (15)	0.0479 (17)	−0.0019 (13)	0.0217 (14)	−0.0011 (13)
O4	0.0310 (17)	0.0235 (16)	0.059 (2)	−0.0014 (14)	0.0162 (15)	0.0056 (15)
N2	0.034 (2)	0.0240 (18)	0.043 (2)	0.0013 (16)	0.0153 (17)	0.0028 (17)
C11	0.026 (2)	0.030 (2)	0.067 (3)	−0.001 (2)	0.015 (2)	0.002 (2)
C12	0.028 (2)	0.044 (3)	0.061 (3)	−0.011 (2)	0.010 (2)	−0.004 (3)
C13	0.033 (3)	0.047 (3)	0.049 (3)	−0.003 (2)	0.011 (2)	0.001 (2)
C14	0.035 (3)	0.035 (2)	0.038 (2)	0.002 (2)	0.009 (2)	0.000 (2)
C15	0.034 (3)	0.034 (3)	0.044 (3)	0.007 (2)	0.018 (2)	0.007 (2)
C16	0.051 (3)	0.051 (3)	0.037 (2)	0.010 (3)	0.018 (2)	0.004 (2)
C17	0.053 (3)	0.055 (3)	0.047 (3)	0.012 (3)	0.031 (3)	0.008 (3)
C18	0.038 (3)	0.048 (3)	0.069 (3)	0.009 (2)	0.034 (3)	0.016 (3)
C19	0.036 (3)	0.026 (2)	0.063 (3)	0.003 (2)	0.021 (2)	0.006 (2)

C20	0.033 (2)	0.024 (2)	0.048 (3)	0.006 (2)	0.022 (2)	0.008 (2)

Geometric parameters (Å, º)

Ni1—O1	2.096 (3)	Ni2—O3	2.041 (3)
Ni1—O1^{i}	2.096 (3)	Ni2—O3^{i}	2.041 (3)
Ni1—O2^{i}	2.029 (3)	Ni2—O4	2.106 (3)
Ni1—O2	2.029 (3)	Ni2—O4^{i}	2.106 (3)
Ni1—N1	2.060 (3)	Ni2—N2	2.053 (3)
Ni1—N1^{i}	2.060 (3)	Ni2—N2^{i}	2.053 (3)
Cl1—C9	1.741 (5)	Cl3—C19	1.737 (5)
Cl2—C7	1.749 (4)	Cl4—C17	1.754 (4)
O1—C1	1.436 (5)	O3—C20	1.319 (4)
O1—H1	0.831 (19)	O4—C11	1.434 (5)
O2—C10	1.312 (4)	O4—H4A	0.836 (19)
N1—C3	1.474 (5)	N2—C13	1.474 (5)
N1—C4	1.282 (5)	N2—C14	1.277 (5)
C1—H1A	0.9700	C11—H11A	0.9700
C1—H1B	0.9700	C11—H11B	0.9700
C1—C2	1.495 (6)	C11—C12	1.505 (6)
C2—H2A	0.9700	C12—H12A	0.9700
C2—H2B	0.9700	C12—H12B	0.9700
C2—C3	1.530 (6)	C12—C13	1.529 (6)
C3—H3A	0.9700	C13—H13A	0.9700
C3—H3B	0.9700	C13—H13B	0.9700
C4—H4	0.9300	C14—H14	0.9300
C4—C5	1.457 (6)	C14—C15	1.450 (6)
C5—C6	1.408 (6)	C15—C16	1.398 (5)
C5—C10	1.416 (6)	C15—C20	1.422 (6)
C6—H6	0.9300	C16—H16	0.9300
C6—C7	1.362 (6)	C16—C17	1.355 (6)
C7—C8	1.370 (7)	C17—C18	1.379 (7)
C8—H8	0.9300	C18—H18	0.9300
C8—C9	1.374 (6)	C18—C19	1.389 (6)
C9—C10	1.410 (5)	C19—C20	1.405 (6)
O1^{i}—Ni1—O1	86.70 (16)	O3—Ni2—O3^{i}	94.75 (15)
O2—Ni1—O1	175.92 (11)	O3—Ni2—O4^{i}	90.54 (11)
O2^{i}—Ni1—O1^{i}	175.92 (11)	O3^{i}—Ni2—O4^{i}	173.47 (11)
O2^{i}—Ni1—O1	89.59 (11)	O3—Ni2—O4	173.47 (11)
O2—Ni1—O1^{i}	89.59 (11)	O3^{i}—Ni2—O4	90.54 (11)
O2^{i}—Ni1—O2	94.17 (15)	O3—Ni2—N2^{i}	96.02 (12)
O2—Ni1—N1^{i}	94.59 (12)	O3—Ni2—N2	86.57 (12)
O2^{i}—Ni1—N1	94.59 (12)	O3^{i}—Ni2—N2^{i}	86.57 (12)
O2^{i}—Ni1—N1^{i}	87.55 (12)	O3^{i}—Ni2—N2	96.02 (12)
O2—Ni1—N1	87.55 (12)	O4—Ni2—O4^{i}	84.44 (16)
N1^{i}—Ni1—O1	87.15 (13)	N2^{i}—Ni2—O4^{i}	89.08 (13)
N1^{i}—Ni1—O1^{i}	90.57 (13)	N2—Ni2—O4^{i}	88.10 (13)

N1—Ni1—O1^{i}	87.15 (13)	N2^{i}—Ni2—O4	88.10 (13)
N1—Ni1—O1	90.57 (13)	N2—Ni2—O4	89.08 (13)
N1^{i}—Ni1—N1	176.86 (19)	N2^{i}—Ni2—N2	176.19 (19)
Ni1—O1—H1	120 (3)	C20—O3—Ni2	116.7 (2)
C1—O1—Ni1	122.2 (3)	Ni2—O4—H4A	118 (3)
C1—O1—H1	108 (3)	C11—O4—Ni2	123.0 (3)
C10—O2—Ni1	119.6 (2)	C11—O4—H4A	111 (3)
C3—N1—Ni1	121.4 (3)	C13—N2—Ni2	121.2 (3)
C4—N1—Ni1	121.7 (3)	C14—N2—Ni2	120.5 (3)
C4—N1—C3	116.6 (4)	C14—N2—C13	117.8 (4)
O1—C1—H1A	109.2	O4—C11—H11A	109.2
O1—C1—H1B	109.2	O4—C11—H11B	109.2
O1—C1—C2	112.2 (4)	O4—C11—C12	112.2 (3)
H1A—C1—H1B	107.9	H11A—C11—H11B	107.9
C2—C1—H1A	109.2	C12—C11—H11A	109.2
C2—C1—H1B	109.2	C12—C11—H11B	109.2
C1—C2—H2A	108.8	C11—C12—H12A	108.7
C1—C2—H2B	108.8	C11—C12—H12B	108.7
C1—C2—C3	114.0 (4)	C11—C12—C13	114.1 (4)
H2A—C2—H2B	107.7	H12A—C12—H12B	107.6
C3—C2—H2A	108.8	C13—C12—H12A	108.7
C3—C2—H2B	108.8	C13—C12—H12B	108.7
N1—C3—C2	113.2 (4)	N2—C13—C12	112.4 (4)
N1—C3—H3A	108.9	N2—C13—H13A	109.1
N1—C3—H3B	108.9	N2—C13—H13B	109.1
C2—C3—H3A	108.9	C12—C13—H13A	109.1
C2—C3—H3B	108.9	C12—C13—H13B	109.1
H3A—C3—H3B	107.7	H13A—C13—H13B	107.9
N1—C4—H4	117.0	N2—C14—H14	117.1
N1—C4—C5	126.1 (4)	N2—C14—C15	125.9 (4)
C5—C4—H4	117.0	C15—C14—H14	117.1
C6—C5—C4	116.9 (4)	C16—C15—C14	117.7 (4)
C6—C5—C10	120.1 (4)	C16—C15—C20	120.5 (4)
C10—C5—C4	122.7 (4)	C20—C15—C14	121.8 (4)
C5—C6—H6	119.8	C15—C16—H16	119.6
C7—C6—C5	120.4 (5)	C17—C16—C15	120.8 (5)
C7—C6—H6	119.8	C17—C16—H16	119.6
C6—C7—Cl2	119.9 (4)	C16—C17—Cl4	120.3 (4)
C6—C7—C8	121.3 (4)	C16—C17—C18	121.2 (4)
C8—C7—Cl2	118.8 (4)	C18—C17—Cl4	118.4 (4)
C7—C8—H8	120.5	C17—C18—H18	120.8
C7—C8—C9	118.9 (4)	C17—C18—C19	118.4 (4)
C9—C8—H8	120.5	C19—C18—H18	120.8
C8—C9—Cl1	118.7 (4)	C18—C19—Cl3	118.4 (4)
C8—C9—C10	123.2 (4)	C18—C19—C20	123.2 (4)
C10—C9—Cl1	118.1 (3)	C20—C19—Cl3	118.4 (3)
O2—C10—C5	123.3 (4)	O3—C20—C15	123.1 (4)
O2—C10—C9	120.7 (4)	O3—C20—C19	121.2 (4)

C9—C10—C5	115.9 (4)	C19—C20—C15	115.8 (4)
Ni1—O1—C1—C2	−53.3 (5)	Ni2—O3—C20—C15	39.1 (5)
Ni1—O2—C10—C5	−37.6 (5)	Ni2—O3—C20—C19	−141.0 (3)
Ni1—O2—C10—C9	144.0 (3)	Ni2—O4—C11—C12	53.0 (4)
Ni1—N1—C3—C2	50.4 (5)	Ni2—N2—C13—C12	−55.5 (5)
Ni1—N1—C4—C5	9.2 (6)	Ni2—N2—C14—C15	−9.6 (6)
Cl1—C9—C10—O2	−4.7 (5)	Cl3—C19—C20—O3	0.0 (6)
Cl1—C9—C10—C5	176.7 (3)	Cl3—C19—C20—C15	179.9 (3)
Cl2—C7—C8—C9	−178.6 (4)	Cl4—C17—C18—C19	−175.4 (3)
O1—C1—C2—C3	69.4 (5)	O4—C11—C12—C13	−66.9 (5)
N1—C4—C5—C6	−169.0 (4)	N2—C14—C15—C16	160.3 (4)
N1—C4—C5—C10	16.1 (7)	N2—C14—C15—C20	−22.0 (7)
C1—C2—C3—N1	−68.4 (5)	C11—C12—C13—N2	68.7 (5)
C3—N1—C4—C5	−177.3 (4)	C13—N2—C14—C15	178.5 (4)
C4—N1—C3—C2	−123.2 (4)	C14—N2—C13—C12	116.4 (4)
C4—C5—C6—C7	−177.4 (5)	C14—C15—C16—C17	178.7 (4)
C4—C5—C10—O2	−0.1 (7)	C14—C15—C20—O3	4.6 (6)
C4—C5—C10—C9	178.4 (4)	C14—C15—C20—C19	−175.3 (4)
C5—C6—C7—Cl2	179.2 (4)	C15—C16—C17—Cl4	174.7 (4)
C5—C6—C7—C8	0.2 (8)	C15—C16—C17—C18	−3.9 (8)
C6—C5—C10—O2	−174.9 (4)	C16—C15—C20—O3	−177.8 (4)
C6—C5—C10—C9	3.6 (6)	C16—C15—C20—C19	2.4 (6)
C6—C7—C8—C9	0.4 (8)	C16—C17—C18—C19	3.2 (7)
C7—C8—C9—Cl1	−178.7 (4)	C17—C18—C19—Cl3	177.5 (4)
C7—C8—C9—C10	1.2 (7)	C17—C18—C19—C20	0.4 (7)
C8—C9—C10—O2	175.4 (4)	C18—C19—C20—O3	177.1 (4)
C8—C9—C10—C5	−3.2 (6)	C18—C19—C20—C15	−3.1 (6)
C10—C5—C6—C7	−2.3 (7)	C20—C15—C16—C17	1.0 (7)

Symmetry code: (i) $-x+1, y, -z+3/2$.

Hydrogen-bond geometry (Å, º)

D—H···*A*	*D*—H	H···*A*	*D*···*A*	*D*—H···*A*
O1—H1···O3	0.84 (3)	1.87 (3)	2.702 (4)	172 (4)
O4—H4*A*···O2^{ii}	0.84 (2)	1.91 (2)	2.736 (4)	168 (4)

Symmetry code: (ii) $x, y-1, z$.